



A Novel Methodology for Inorganic Scaling Simulation: Multiphase Flow and Real Water Solutions with a Fickian Approach

Rodrigo. S. Maciel¹, João N. E. Carneiro¹, André F. F. Souza², Danielle Monteiro³, Vidar Gunnerud³

¹ISDB Flowtech, corresponding author: rodrigo.simoes@isdbflowtech.com

²Petrobras

³Solution Seeker

Abstract

Inorganic scaling on production equipment such as solid-containing screens, slide sleeve valves, and tubing poses a flow assurance problem. Scaling obstructs flow by reducing open area, leading to increased head loss and, in severe cases, complete production blockage. Carbonatic scaling is influenced by local pressure, temperature, and the presence of various ionic species at differing concentrations. Changes in the aqueous composition of CO₂, coupled with pressure drops, can alter the saturation index and precipitation rate, initiating scaling. Additionally, scaling is influenced by turbulence intensity, which affects the transport of crystals or chemical species towards the wall. This paper proposes a novel methodology for modeling and simulating calcium carbonate scaling in a one-dimensional context. It employs a geochemical simulator coupled with a Fickian transport methodology, tailored for multiphase flow scenarios involving oil, gas, and water. The treatment of multiphase flow as a mixture or segregated flow system is determined through analysis of Reynolds and Froude numbers. Using this approach, the scaling rate on a pipe wall was simulated, demonstrating good agreement with field and literature observations. Specifically, the results shows that scaling increases with flow rate, pressure head, CO₂ flash, and temperature.

Keywords

Inorganic scaling; Carbonatic scaling; Flow assurance; Geochemical simulator; Multiphase flow.

Introduction

In the oil and gas industry, the challenge of inorganic scaling within production equipment is paramount, impacting flow dynamics and potentially leading to production blockages. Carbonate scaling, particularly sensitive to environmental factors, poses a significant concern due to its intricate nature.

Studies have been dedicated to investigating the mechanisms and factors contributing to the deposition of calcium carbonate (CaCO₃) on metal surfaces exposed to environments containing carbon dioxide (CO₂). Numerical models and simulations have been widely employed to deepen the understanding of the CaCO₃ precipitation process, as exemplified by [2], who investigated the implications of the oily phase and CO₂ degassing on carbonate precipitation. In the field of scaling modeling, [6] proposed a rigorous kinetic model to simulate calcium carbonate deposit formation in turbulent flow environments, considering diffusional transport and crystallization kinetics. Their simplified approach, showing results within 10% accuracy, considers a Fickian transport solution for a simplified system with CO₂-H₂O-Ca⁺². [3] introduced a methodology for assessing scaling potential during CO₂-WAG injection in carbonate reservoirs, aiding cost estimation and risk reduction. By incorporating geochemical simulation, they identified the least susceptible

recovery method and mitigated overestimation of scaling risk, informing project decisions and injection design. [1] investigated scaling tendencies under water evaporation and CO₂ dissolution using coupled geochemical and compositional wellbore simulators. They explored the effects of water evaporation and CO₂ dissolution on scaling in oil and gas wells by numerically solving a mass transport equation, transporting the precipitated CaCO₃ toward the adhesion wall, the precipitation was estimated by a geochemical solver.

Addressing the intricate interplay of factors influencing inorganic scaling, this paper introduces a novel methodology for modeling and simulating calcium carbonate scaling within a one-dimensional framework. It considers multiphase flow (oil, gas, and brine) with real composition formation water, accounting for the effects of temperature, pressure, and CO₂ solubilization, including its flash due to pressure head. By integrating a geochemical simulator with a tailored Fickian transport methodology, the approach accommodates multiphase flow scenarios and the intricate effects of CO₂ on the precipitation reaction.

Through rigorous application of the proposed methodology, the study simulates scaling rates on pipe walls, aligning well with field observations and existing literature. This comprehensive framework sheds light on the pivotal role of multiphase flow

dynamics and geochemical interactions, laying a robust foundation for further advancements in flow assurance strategies.

Methodology

To achieve the goal of modeling and simulating the scaling rate, we developed a methodology based on [7] and [5]. However, the current approach allows us to consider a real water solution, in contrast to [7], which only considers a simplified H₂O-CO₂-Ca system.

The full methodology is depicted in Fig.1, illustrating the inputs: local oil, gas, and water volumetric flow rates, temperature, pressure, hydraulic diameter, and water composition. We employed a geochemical computational package (Reaktor[®]) to model and simulate the equilibrium state of an ionically saturated formation water (Ca²⁺, K⁺, Sr²⁺, Ba²⁺, Mg²⁺, Na⁺, Cl⁻, SO₄²⁻, Fe²⁺, HCO₃⁻).

The geochemical model receives the ionic concentration and the CO₂ molar fraction to account for the solution gas solubility and output the precipitates molarity of CaCO₃, its saturation index (SI), and the equilibrium pH.

In parallel, the procedure set forth in [5] was applied to compute the mixture properties such as velocity, specific mass, viscosity and mixture Reynolds. According to [8], based on the Reynold and Froud mixture number, if the flow fits segregated flow configuration, the further calculation was based on water velocity and wet diameter, else, the flow is modeled as mixture flow. Then, CaCO₃ diffusivity was property obtained as function of Reynolds, Sherwood and Smith number according to [9].

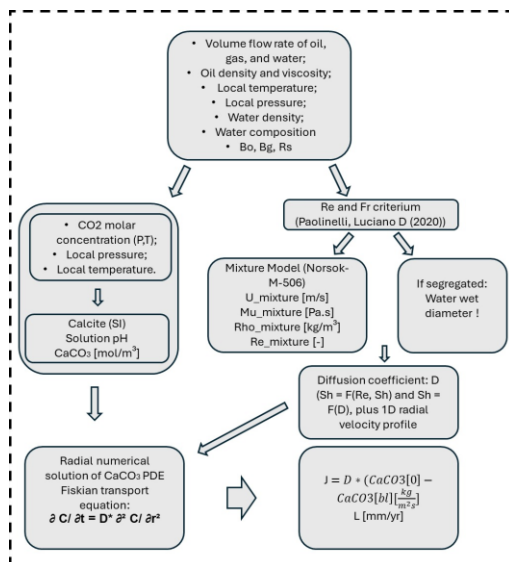


Figure 1. Flowchart of inorganic scaling models.

Finally, the concentration profile was obtained by the numerical solution of a diffusion equation, as presented by [7], and the wall mass flow rate [kg/m²s] as well as the scaling rate in [mm/yr] were estimated.

Simulated Conditions

To analyze the output, a generic formation water assumption was made, similar in magnitude to that typically observed in a Brazilian pre-salt reservoir. Table 1 lists the main chemical species along with their concentrations. Additionally, two molar fractions of CO₂ were considered.

Table 1. Insert the Table title.

Ionic specie	Concentration
H ₂ O	1[kg]
Ca ²⁺	2000 [mg/kg]
K ⁺	2000 [mg/kg]
Sr ²⁺	200[mg/kg]
Ba ²⁺	1[mg/kg]
Mg ²⁺	200[mg/kg]
Na ⁺	30000[mg/kg]
Cl ⁻	60000[mg/kg]
SO ₄ ²⁻	1000[mg/kg]
Fe ²⁺	0 [mg/kg]
HCO ₃ ⁻	2000[mg/kg]

For the simulation, local conditions were assumed with in situ oil volumetric flow rate of 3000 m³/day, gas volumetric flow rate of 800 m³/day, a water flow rate of 38 m³/day, oil viscosity of 0.05 Pas, density of 600 kg/m³, and a hydraulic diameter of 6 inches.

Results and Discussion

To validate the geochemical model, simulations were conducted, and the results are outlined in Figure 2. The model enables simulation of the effects of temperature and pressure on a system involving pure water and CO₂. It demonstrates good agreement with experimental results, depicting an increase in pH with pressurization and temperature elevation. This effect is indirectly associated with CaCO₃ precipitation, as pressure drop tends to increase pH due to CO₂ release. Additionally, temperature tends to elevate CO₂ fugacity, thereby accelerating its release and increasing pH.

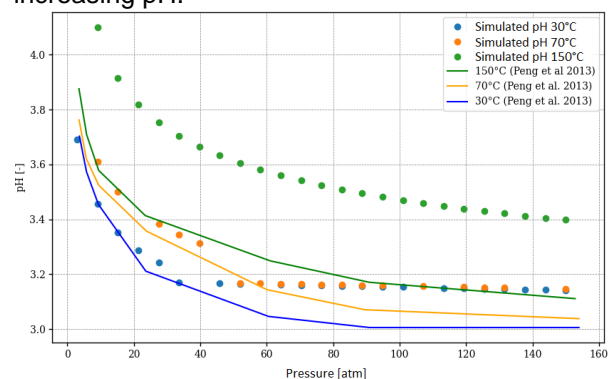


Figure 2. pH simulated vs. experimental valuer for a pure water and 100% CO₂ system.

However, the model tends to underestimate the effect of temperature on pH, due to the high CO₂ concentration, since this effect was not observed for smaller CO₂ molar concentrations (~10%). Figures 3 and 4 display the pH surfaces for a specified temperature and pressure range. In Fig. 3, the simulation was conducted using the

concentrations listed in Table 1 and a 10% CO₂ molar fraction, while in Fig. 4, the simulation was performed with a 1% CO₂ molar fraction. In both graphs, pH increases with pressure and temperature, demonstrating the effect of CO₂ solubility influenced by pressure and temperature.

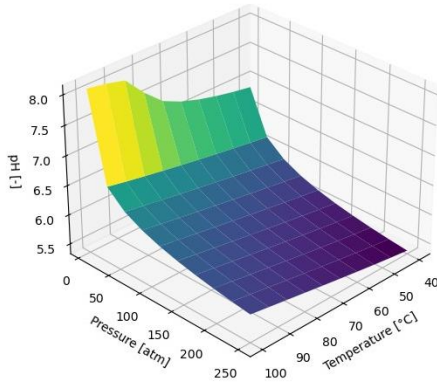


Figure 3. pH surface for 10% CO₂ molar fraction.

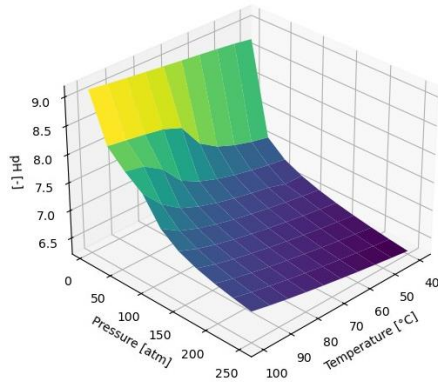


Figure 4. pH surface for 1% CO₂ molar fraction.

Figures 5 and 6 depict SI surfaces for a specified temperature and pressure range. Where $SI = \log(SR)$, being the SR the saturation ratio, where $SR = \frac{a(Ca^{2+}) \cdot a(CO_3^{2-})}{K_{ps}}$, with K_{ps} representing the solubility product constant ([7]). These terms within braces correspond to the chemical activity and change with the presence of other ions adverse to the reaction, in a more realistic brine.

In Fig. 5, the simulation utilized the concentrations listed in Table 1 and a 10% CO₂ molar fraction, while in Fig. 6, the simulation was conducted with a 1% CO₂ molar fraction. Similarly to the pH behavior, in both graphs, the saturation index (SI) increases with pressure reduction and temperature increment, illustrating the impact of these variables on CO₂ solubility and CaCO₃ precipitation behavior.

The phase volumetric flow rates were described in the section of simulated conditions, in methodology.

Comparing Figure 7 and 8, the effect of CO₂ molar fraction becomes apparent. In the case of a 10% molar fraction, the highest scaling rate occurs with

the smallest CO₂ molar fraction. This phenomenon is attributed to the increased pH and SI observed with a lower amount of CO₂. Furthermore, the influence of temperature and pressure on scaling rate aligns with the observations outlined in the analysis of pH and SI.

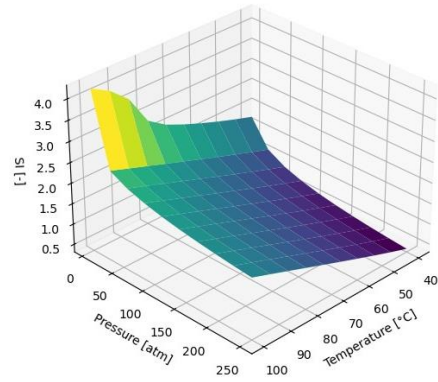


Figure 5. SI surface for 10% CO₂ molar fraction.

Figures 7 and 8 display scaling rate surfaces for a specified temperature and pressure range, considering the concentrations of species listed in Tab.1.

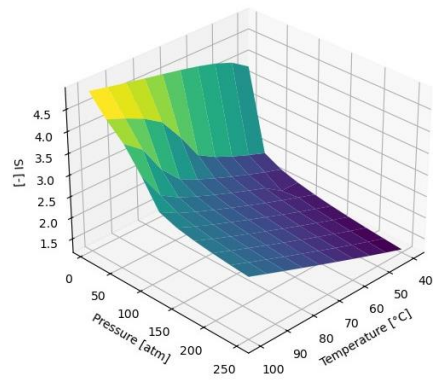


Figure 6. SI surface for 1% CO₂ molar fraction.

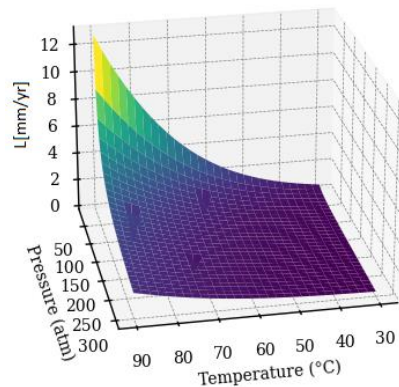


Figure 7. Scaling rate surface for 10% CO₂ molar fraction.

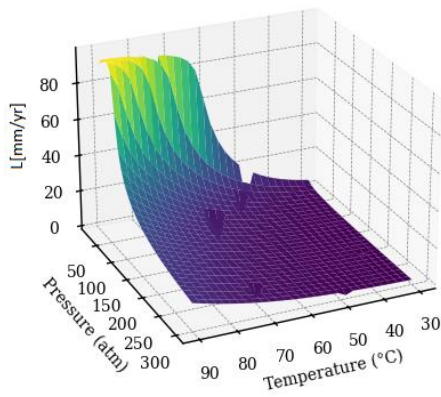


Figure 8. Scaling rate surface for 1% CO₂ molar fraction.

Finally, Fig. 10 shows scaling rate for a range of oil flow rate, showing the effect of the transport model, and pressure for a temperature of 90°C.

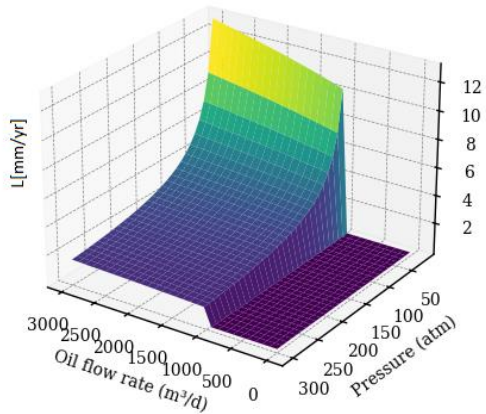


Figure 10. Scaling rate surface for 10% CO₂ molar fraction. Effect of oil flow rate.

Here's the corrected version:

At low flow rates, the model reduces the turbulent diffusion of the concentration field, as illustrated in the effect of oil flow rate above, reducing the scaling rate.

The model accounts for the highest scaling rate at lower pressure regions along with increasing oil flow rate.

Then, we test the physical model with a generic thermohydraulic profile along the well. We input local oil, gas, and water flow rates, pressure, and temperature, along with a constant 10% CO₂ molar fraction. Fig. 11 and 12 show scatter plots of scaling rates over a time series at the bottom hole and wellhead sites, as a function of temperature (left) and pressure (right), and total flow rate. The blue-to-red scale indicates the highest scaling rate conditions at high flow rates, temperatures, and smallest total pressures, demonstrating the model behavior closer to real conditions.

Using bottom hole, wellhead, and upstream data, the scaling rate is presented in Fig. 13. These data were used to train a neural network for a linear regression, and a random forest model. Fig. 14 compares the scaling physical model against the

fitting of the linear regression and random forest models.

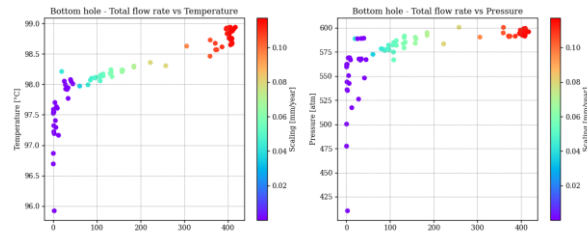


Figure 11. Scaling rate surface for 10% CO₂ molar fraction. Effect of total flow rate, pressure and temperature at bottom hole.

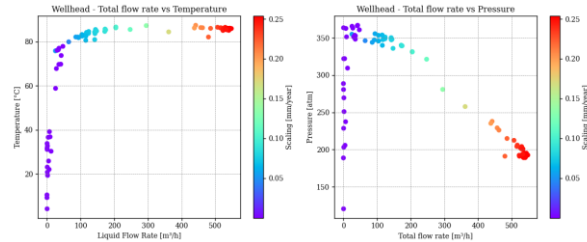


Figure 12. Scaling rate surface for 10% CO₂ molar fraction. Effect of total flow rate, pressure and temperature at bottom wellhead.

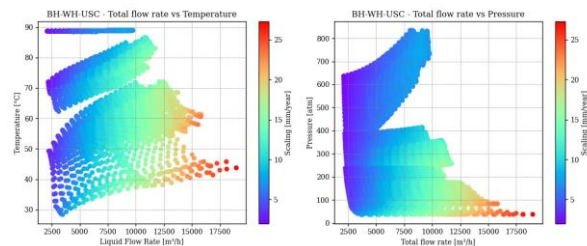


Figure 13. Scaling rate surface for 10% CO₂ molar fraction. Effect of total flow rate, pressure and temperature at bottom, wellhead and upstream chock.

These comparisons demonstrate that the physical model could be employed to generate synthetic training and testing databases for training and testing AI models, achieving sufficiently good fitting quality.

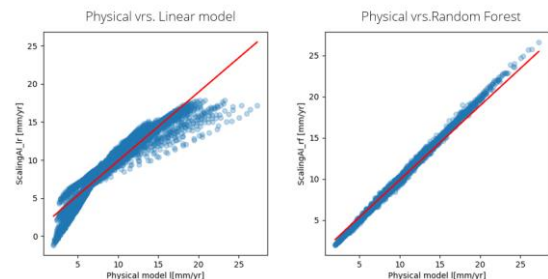


Figure 14. Physical model vrs. linear model (left) and random forest (right).

Furthermore, the model could be integrated into real-time monitoring systems (applying the physical model or an AI trained model) to provide early warnings of potential scaling issues, allowing operators to take corrective actions before production is significantly affected.

Conclusions

In conclusion, the geochemical model's validation through simulations, as outlined in Fig.1, demonstrates its efficacy in simulating the impact of temperature and pressure on systems involving pure water and CO₂. The observed pH increases with pressurization and temperature correlates indirectly with CaCO₃ precipitation, driven by pressure-induced CO₂ release and temperature-driven CO₂ fugacity rise. Figs.2 through 4 depict pH surfaces for varying CO₂ molar fractions, showcasing the influence of pressure and temperature on pH and CO₂ solubility. Additionally, Figs. 5 through 8 illustrate saturation index (SI) and scaling rate surfaces, underscoring the effects of CO₂ molar fraction, temperature, and pressure on scaling behavior. Finally, Fig. 10 demonstrates the scaling rate's sensitivity to oil flow rate, highlighting the transport model's impact and pressure's role at lower pressure regions.

With the application of a more realistic dataset, the physical model demonstrates its capabilities in estimating the scaling rate along a producing oil well. Finally, it was able to estimate high scaling rate regions and observe cluster zones highlighting these regions. Additionally, the output of the scaling model was used to feed an AI training network, resulting in good fitting quality.

Acknowledgments

The authors would like to thank PETROBRAS for the permission to publish this work, as well as the Brazilian National Petroleum Agency (ANP) for the financial support ("Compromisso de Investimentos com Pesquisa e Desenvolvimento").

References

[1] Coelho, Fernando MC, Kamy Sepehrnoori, and Ofodike A. Ezekoye. "Coupled geochemical and compositional wellbore simulators: A case study on scaling tendencies under water evaporation and CO₂ dissolution." *Journal of Petroleum Science and Engineering* 202 (2021): 108569.

[2] Cosmo, Rafael de P., Fabio de A. Ressel Pereira, Daniel da C. Ribeiro, Wagner Q. Barros, and André L. Martins. "Estimating CO₂ degassing effect on CaCO₃ precipitation under oil well conditions." *Journal of Petroleum Science and Engineering* 181 (2019): 106207.

[3] de Souza, Ana Paula, and Eric Mackay. "Modelling of CO₂ and seawater injection in carbonate reservoirs to evaluate inorganic scaling risk." In *SPE International Oilfield Scale Conference and Exhibition?*, p. D011S001R004. SPE, 2014.

[5] Olsen, Stein. "CO₂ corrosion prediction by use of the Norsok M-506 model-guidelines and limitations." In *NACE CORROSION*, pp. NACE-03623. NACE, 2003.

[6] Peng, Cheng, John P. Crawshaw, Geoffrey C. Maitland, JP Martin Trusler, and David Vega-Maza. "The pH of CO₂-saturated water at temperatures between 308 K and 423 K at pressures up to 15 MPa." *The Journal of Supercritical Fluids* 82 (2013): 129-137.

[7] Segev, Raviv, David Hasson, and Raphael Semiat. "Rigorous modeling of the kinetics of calcium carbonate deposit formation." *AIChE Journal* 58, no. 4 (2012): 1222-1229.

[8] Paolinelli, Luciano D. "A comprehensive model for stability of dispersed oil-water flow in horizontal and inclined pipes." *Chemical Engineering Science* 211 (2020): 115325.

[9] Maragkos, Georgios, and Tarek Beji. "Review of convective heat transfer modelling in cfd simulations of fire-driven flows." *Applied Sciences* 11, no. 11 (2021): 5240.